Lateral Diffusion of an Adsorbate at Chromatographic Octadecylsiloxane/Water Interfaces of Varying Hydrocarbon Density

John M. Kovaleski and Mary J. Wirth*

Department of Chemistry & Biochemistry, University of Delaware, Newark, Delaware 19716

Received: January 23, 1997; In Final Form: May 6, 1997[⊗]

The lateral diffusion of acridine orange was investigated at the interface of water and octadecylsiloxane (C_{18}) monolayers of varying hydrocarbon density. The surfaces examined ranged from 24% to 100% of a sterically complete monolayer of 3.5 μmol/m^2 in alkane coverage. Fluorescence recovery after photobleaching was used to measure the lateral diffusion coefficient. Acridine orange is a fluorophor known to reside at the water/hydrocarbon interface, negligibly adsorbing to bare silica. Its diffusion coefficient was found to decrease 500-fold as the surface coverage was reduced 4-fold. By use of effective medium and percolation theory, the strong density dependence was attributed to decreased contiguity of hydrocarbon at lower coverages. The temperature dependence of the lateral diffusion coefficient showed that the decease in diffusion rate at lower coverage was entirely due to an increase in the entropic barrier, pointing to percolation as the mechanism of diffusion.

Introduction

Liquid chromatography is one of the most widely used separation techniques, yet there are still many questions concerning the organization and dynamics of the stationary phase structure. Various spectroscopic techniques have been used to characterize these phases including NMR,[1−5] Fourier transform infrared (FTIR),[4−7] Raman,[8] X-ray photoelectron spectroscopy (XPS),[9,10] and fluorescence[11−14] measurements. An additional method that has proved useful in probing chromatographic monolayers is fluorescence recovery after photobleaching.[15−17] This method measures transport rate of a probe molecule over distances greater than micrometers.

Acridine orange is the probe chosen for these studies because it is a fluorescent adsorbate that has been well characterized at chromatographic interfaces.[18−24] Fluorescence anisotropy measurements indicate that it is highly oriented at hydrocarbon/water interfaces,[18−24] as depicted in Figure 1. Additionally, it has been found that acridine orange negligibly adsorbs to bare silica[18] and does not partition into the hydrocarbon phase.[20] Previous studies have shown that the lateral diffusion coefficient of acridine orange at liquid hydrocarbon/water interfaces decreases with increasing interfacial roughness.[25] The lateral diffusion coefficient was found to be an order of magnitude smaller for the chromatographic C_{18}/water interface, where C_{18} indicates a monolayer of covalently bonded dimethyloctadecylsiloxane.[25]

Physical insight into the origin of the large decrease in lateral diffusion for the chromatographic surface is gained through the temperature dependence of the lateral diffusion coefficient through an Arrhenius relation

$$\ln D = \ln D_0 - (\Delta U/RT) \qquad (1)$$

where D_0 is the diffusion coefficient in the absence of the activation barrier, ΔU. An Arrhenius plot of the lateral diffusion coefficient revealed very different behavior for the liquid dodecane/water and C_{18}/water interfaces, where the former exhibits a 36 kJ/mol activation barrier while the latter exhibits only a 7 kJ/mol activation barrier but a large entropic barrier.[26] The physical origin of the 7 kJ/mol activation barrier was speculated to be either disengaging of the cationic probe from anionic sites on the silica substrate or displacement of the probe from C_{18} sites to C_1 sites. The C_1 sites had been introduced by post reacting the C_{18} surface with chlorotrimethylsilane, a procedure often called "endcapping" that is intended to minimize the exposure of the silica substrate. The origin of the entropic barrier was postulated as either unfavorable sites owing to exposed silica substrate or roughness features at the C_{18}/water interface, either of which would restrict the sites accessible to the diffusing adsorbate.

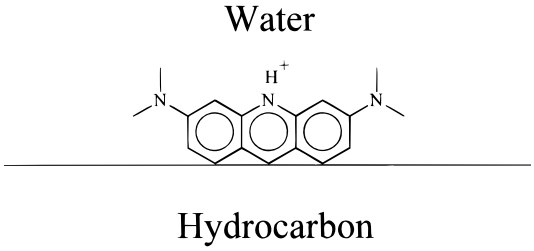

Figure 1. Orientation of acridine orange at water/hydrocarbon interfaces.

The purpose of the present work is to investigate further the physical origin of the lateral diffusion of acridine orange at C_{18}/water interfaces. Endcapping is eliminated to simplify the surfaces and C_{18} coverage is varied to explore how a reduction in hydrocarbon surface area influences lateral diffusion.

Experimental Section

Acridine Orange (90+%) was obtained from Eastman Kodak and was purified by passage through a silica column using a methanol mobile phase. The water was distilled and then deionized to 18 MΩ cm using a Barnstead E-pure system. The water was further passed through a 0.2 μm particle filter to remove dust. These procedures removed ionic, nonpolar, and surface active impurities.

The substrates for the varying density monomeric C_{18} surfaces were fused silica plates purchased from Esco Products. The plates were heated in nitric acid to remove impurities before derivatization. *n*-Heptane, the solvent used for synthesizing the full coverage monomeric surface, was obtained from Fisher and purified by passage through a silica column to remove polar

* Corresponding author.
⊗ Abstract published in *Advance ACS Abstracts,* July 1, 1997.

S1089-5647(97)00300-3 CCC: $14.00

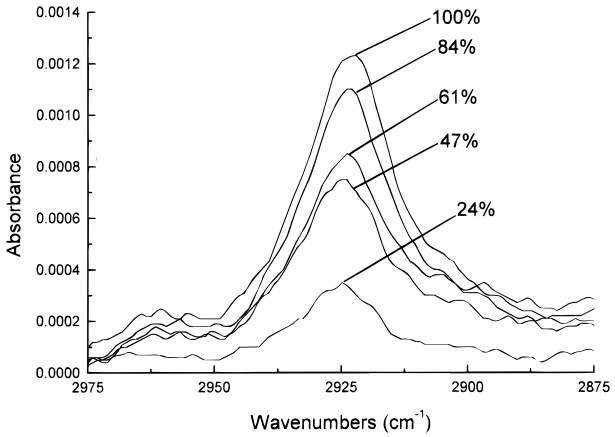

Figure 2. FTIR spectra illustrating the asymmetric methylene stretch for the varying density monomeric C_{18} surfaces.

impurities. The silanization reagent, chlorodimethyloctadecylsilane (95%), and catalyst, *n*-butylamine (98%), were obtained from Aldrich and used as received. The reaction was conducted as reported previously,[18] but without endcapping. For the lower density surfaces, slight variations were made in the derivatization procedure. Toluene, obtained from Fisher, was purified through silica and used as the reaction solvent, and the amount of reagent added to the system was reduced. Finally, the reaction time was varied to obtain the surface coverage desired. After derivatization, all surfaces were rinsed with toluene and acetone. The surface coverages were measured using a Mattson Galaxy 5000 Series FTIR.

The optical arrangement for the lateral diffusion experiments has been described previously.[15,25] A Coherent Innova 400 argon ion laser at 488 nm was used as the excitation source. A half-wave plate and Glan-laser prism were used to ensure that the beam was polarized in the plane of the interface. A Pockels cell (Quantum Technology) followed by a second Glan-laser prism allowed the beam to be switched between bleach and probe intensities without changing polarization. The beam was then spatially filtered and collimated before passage through the desired Ronchi ruling (Applied Image, Inc.). Rulings of 10−400 μm were used in this study, depending upon the rate of diffusion. Imaging of the grating onto the sample cell was then accomplished as described previously.[15]

For all lateral diffusion experiments, acridine orange was adsorbed from a 6 nM aqueous solution. The acridine orange solution was replaced with pure water before starting the lateral diffusion experiment. This minimized any contribution to fluorescence recovery from additional adsorption of acridine orange from solution during the data acquisition. The mobile phase temperature was controlled using a Neslab temperature bath and was monitored using a thermocouple (Omega Engineering, Inc.) placed near the interface. The data acquisition electronics and software were the same as those used previously.[15,25] MicroCal Origin was used for data analysis and plotting.

Results and Discussion

The FTIR spectra for each of the varying density monomeric C_{18} surfaces are shown in Figure 2. The relative surface coverages were determined to be 24%, 47%, 61%, 84%, and 100% of a full monolayer. The full monolayer was determined to have the expected surface coverage of 3.5 μmol/m^2, which is approximately the steric limit of dimethyloctadecylsiloxane chains. The corresponding area per chain is listed in Table 1 for each surface coverage, with the areas ranging from 48 to 210 Å^2/chain. An individual C_{18} chain lying flat on a surface would cover an area of approximately 78 Å^2, based on the 1.54 and 1.1 Å C−C and C−H bond distances, respectively, and the nearly tetrahedral angles. On the average, therefore, it is not possible for the lower coverage surfaces to avoid significant exposure of the silica substrate. The small shift in the infrared spectrum indicates an increase in population of gauche conformations as coverage is decreased. The gauche population can be calculated from the known spectral position of the methylene stretch when the hydrocarbon is in all trans conformations (2920 cm^{-1}) and the corresponding spectral position for the liquid hydrocarbon at room temperature (2928 cm^{-1}).[27] For the 3.3 kJ/mol energy difference between gauche and trans conformations, the thermal gauche population would be 20%. Assuming a linear shift with population between the two extremes, the calculated gauche populations are listed in Table 1.

TABLE 1: Summary of Hydrocarbon Coverage, Area per C_{18} Chain, Methylene Stretch Peak Position, Calculated Percentage of Gauche Bonds, and Lateral Diffusion Coefficient of Acridine Orange at 20 °C

surface coverage (μmol/m^2)	fraction of surface coverage	average area (Å^2/ chain)	methylene stretch peak (cm^{-1})	% of gauche bonds	diffusion coefficient $\times 10^9$ (cm^2/s)
0.8 ± 0.2	0.24 ± 0.04	210 ± 40	2924.8	12	1.1 ± 0.1
1.6 ± 0.3	0.47 ± 0.07	100 ± 20	2924.6	12	18 ± 3
2.1 ± 0.2	0.61 ± 0.06	79 ± 8	2923.6	9	75 ± 4
2.9 ± 0.4	0.84 ± 0.12	57 ± 9	2923.5	9	350 ± 20
3.5 ± 0.3	1.00 ± 0.08	48 ± 5	2922.7	7	510 ± 20

Representative raw data for the fluorescence recovery after photobleaching for acridine orange at a monomeric C_{18}/water interface are shown in Figure 3. All recovery curves fit well to a single-exponential decay with time constant, τ.

$$\tau = d^2/(4\pi^2 D) \qquad (2)$$

For all systems, at least two grating spacings, d, were used to determine the diffusion coefficient, D. This ensured that the data recovery arose from lateral diffusion rather than some other type of phenomenon such as readsorption from the mobile phase. The size of the gratings used for each surface was dependent upon the rate of diffusion at that particular interface. A summary of the diffusion coefficient obtained at each surface at 20 °C is listed in Table 1. From the data, it can be seen that the diffusion coefficient of acridine orange decreased 500-fold as the surface coverage was lowered over the density range studied.

The density dependence of lateral diffusion of a membrane probe in a Langmuir monolayer as a function of monolayer density has been studied and found to be described by effective-medium theory.[28,29] Effective-medium theory treats the monolayer as having two regions of differing diffusivity. In the case of Langmuir monolayers, liquid and gas phases coexist. Percolation theory also describes lateral diffusion in phase-separated monolayers and applies when the unfavorable areas are strictly excluded, resulting in a threshold coverage of 67% required for diffusion to occur.[30] The threshold coverage is high because continuous paths across the surface are required for diffusion.

To test the applicability of effective-medium and percolation theories, Figure 4 shows a plot of the lateral diffusion coefficient of acridine orange vs fractional coverage of a monolayer. The solid curve is generated by the Bruggeman−Landauer equation from effective-medium theory,[30] shown below

$$\frac{D_x}{D_{\text{full}}} = (x - 0.5)(1 - r) + \sqrt{(x - 0.5)^2(1 - r) + r} \qquad (3)$$

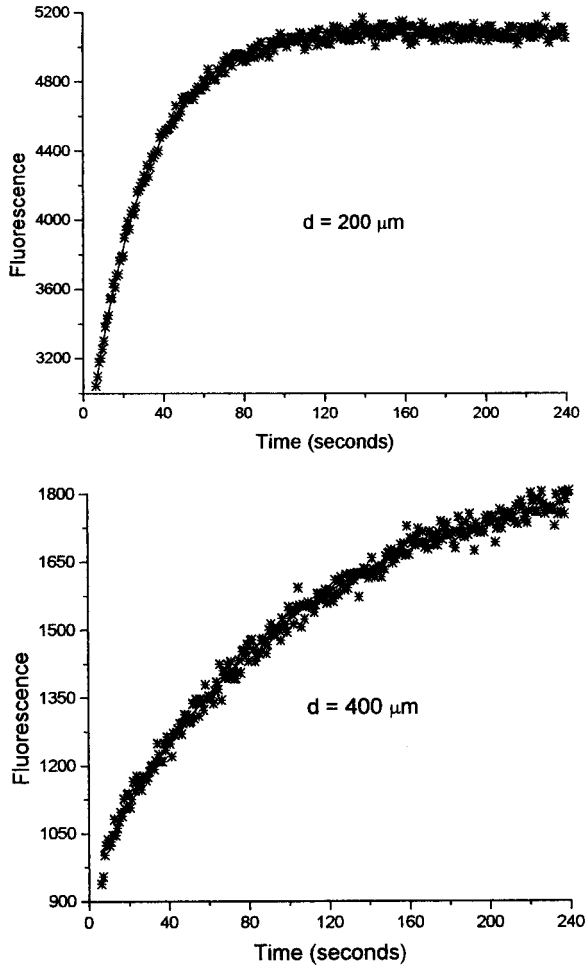

Figure 3. Sample fluorescence recovery after photobleaching data for the monomeric C_{18}/water interface. For this particular system the 200 and 400 μm gratings were used.

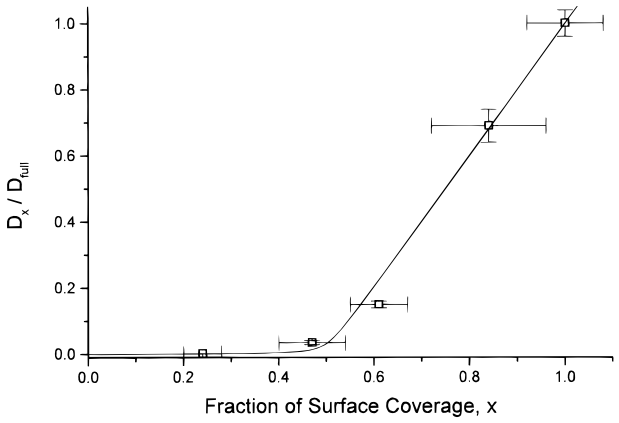

Figure 4. Relation between lateral diffusion coefficient at room temperature and the hydrocarbon coverage of the silica surface.

D_x represents the diffusion coefficient at the fraction of surface coverage, x, and D_{full} is the diffusion coefficient at full coverage. The term r is a ratio which takes into account the diffusion coefficients within the two regions of differing diffusivity and the probability of the probe residing in the barrier region. For the data presented in Figure 4, the fit is excellent for the case of $r = 0.001$. Percolation theory does not fit the data: no threshold is evident and the diffusion coefficient at 67% coverage is quite high. These results indicate that the coverage dependence of the lateral diffusion of acridine orange can be explained by decreased contiguity of the hydrocarbon monolayer as the coverage is lowered and that acridine orange is either

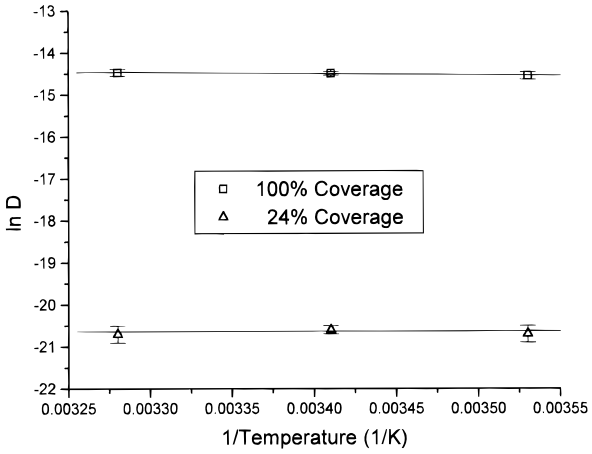

Figure 5. Arrhenius plot for the lateral diffusion coefficient of acridine orange at the 100% and 24% coverage monomeric C_{18}/water interfaces.

TABLE 2: Temperature-Dependence Data for the 100% and 24% Coverage Surfaces[a]

100% coverage surface		24% coverage surface	
temp (°C)	diffusion coefficient (cm^2/s)	temp (°C)	diffusion coefficient (cm^2/s)
10	$(4.8 \pm 0.4) \times 10^{-7}$	10	$(1.0 \pm 0.2) \times 10^{-9}$
20	$(5.1 \pm 0.2) \times 10^{-7}$	20	$(1.1 \pm 0.1) \times 10^{-9}$
32	$(5.2 \pm 0.4) \times 10^{-7}$	32	$(1.0 \pm 0.2) \times 10^{-9}$
ΔU^b	3 ± 3 kJ/mol	ΔU^b	0 ± 5 kJ/mol
$\ln D_0$	-13.5 ± 0.5	$\ln D_0$	-21 ± 2
D_0	$(2 \pm 1) \times 10^{-6}$ cm^2/s	D_0	$< 6 \times 10^{-9}$ cm^2/s

[a] Thermodynamic parameters were obtained from the Arrhenius plots in Figure 5. [b] Activation energy.

able to diffuse across the silica sites at a 1000-fold slower rate or is 1000 times less likely to be located at one of these sites.

An independent test of whether diffusion is controlled by effective medium vs percolation behavior is the temperature dependence of the lateral diffusion coefficient. If the bare silica sites are inaccessible, as in percolation behavior, the entropic barrier would increase significantly as the density were lowered. The temperature dependence of the lateral diffusion coefficient is reported for the highest and lowest surface coverages. The temperature dependences of the intermediate densities were changed upon measurement because elevated temperatures caused irreversible decreases in the diffusion coefficients due to irreversible decrease in coverage. The change in diffusion coefficient with coverage, as shown in Figure 4, is maximum at intermediate coverages, explaining why irreversible change was only a problem at intermediate coverages. The Arrhenius plots for the two extreme surface coverages are shown in Figure 5, exhibiting simple behavior over the 10−32 °C range studied. The recovered thermodynamic parameters are listed in Table 2. From the slopes, $\Delta U/R$, the activation barrier, ΔU, is calculated to be within kT of zero for both cases: 3 ± 3 and 0 ± 5 kJ/mol for the 100% and 24% coverages, respectively.

The activation barriers for both extreme coverages are smaller than the activation barrier that had been previously observed for the endcapped surface of 100% coverage: 7 ± 1 kJ/mol.[26] This result eliminates silica charge as the origin of the activation barrier because the non-endcapped surfaces would have even higher surface charges. The fact that the activation barrier virtually disappears points to the alternative suggestion for the activation barrier on the endcapped surface: different energies of interaction with the methyl groups vs the octadecyl groups. The differences in interaction energy are on the order of a few kJ/mol, as estimated by theory[31] and from spectral shifts in

Shpol'ski matrices.[32] The small barrier for these non-endcapped surfaces supports the conclusion that the lateral diffusion of acridine orange does not require crossing a significant length of hydrated, bare silica because this would demand a different activation barrier at low coverage than at maximum coverage. The barrier is unlikely to be zero, and the origin of the small barrier cannot be determined from these measurements. One speculation is that it could be the change in dispersion energy as the molecule diffuses across the amorphous hydrocarbon surface.

The small slope and large negative intercept establish that the lateral diffusion of acridine orange is controlled entropically at the C_{18}/water interface for both the high and low coverages. The increase in entropic barrier with decreasing density entirely accounts for the drastically reduced diffusion coefficient. The entropic barrier indicates that the bare silica sites are inaccessible. Physically, this agrees with the percolation model of lateral diffusion, where the probe must search for paths of contiguity to diffuse laterally over the distances on the order of the grating spacing. The thermodynamic result thus shows that the lack of a threshold in the density dependence of the lateral diffusion is not a criterion for eliminating percolation as the interpretation. A plausible reason for the absence of a threshold is that the two-dimensional arguments used to arrive at the 67% threshold do not apply to these monolayers. The chromatographic C_{18} monolayer is three-dimensional, with a thickness that decreases with coverage, thereby reducing the threshold at which the monolayer would become discontiguous. The increasing proportions of gauche conformations shown in Table 1 are experimental indication that the constituent hydrocarbon chains respond to the decrease in coverage.

The strong density dependence of the lateral diffusion of acridine orange contrasts with the behavior of rubrene, reported by Hansen and Harris.[17] Rubrene, or 5,6,11,12-tetraphenylnaphthacene, is a symmetric and hydrophobic molecule that is 25% larger than acridine orange. Rubrene is presumed to reside in the hydrocarbon interphase. One would expect that the diffusion of this hydrophobic probe would also be sensitive to contiguity; however, for an approximately 2-fold drop from maximum hydrocarbon coverage, only a slight decrease in the diffusion coefficient was observed: $4.0\ (\pm 0.4) \times 10^{-9}$ and $2.9\ (\pm 0.4) \times 10^{-9}$ cm^2/s for the higher and lower density, respectively. The diffusion coefficient of acridine orange dropped 30-fold over this range. A possible explanation for the difference in behavior is that the diffusion coefficient of rubrene is already so low that the increased entropic barrier does not significantly affect the diffusion coefficient.

Acknowledgment. This work was supported by the National Science Foundation under Grant CHE-91-13544. Fellowship support (to J.M.K.) from the University of Delaware is gratefully acknowledged.

References and Notes

(1) Sentell, K. B. *J. Chromatogr.* **1993,** *656,* 231.
(2) Kelusky, E. C.; Fyfe, C. A. *J. Am. Chem. Soc.* **1986,** *108,* 1746.
(3) Bayer, E.; Paulus, A.; Peters, B.; Laupp, G.; Reiners, J.; Albert, K. *J. Chromatogr.* **1986,** *364,* 25.
(4) Koehler, J.; Chase, D. B.; Farlee, R. D.; Vega, A. J.; Kirkland, J. J. *J. Chromatogr.* **1986,** *352,* 275.
(5) Gilpin, R. K. *J. Chromatogr.* **1993,** *656,* 217.
(6) Sander, L. C.; Callis, J. B.; Field, L. R. *Anal. Chem.* **1983,** *55,* 1068.
(7) Sagliano, N.; Hartwick, R. A.; Patterson, R. E.; Woods, B. A.; Bass, J. L.; Miller, N. T. *J. Chromatogr.* **1988,** *458,* 225.
(8) Thompson, W. R.; Pemberton, J. E. *Anal. Chem.* **1994,** *66,* 3362.
(9) Barrett, D. A.; Brown, V. A.; Davies, M. C.; Shaw, P. N. *Anal. Chem.* **1996,** *68,* 2170.
(10) Brown, V. A.; Barrett, D. A.; Shaw, P. N.; Davies, M. C.; Ritchie, H. J.; Ross, P.; Paul, A. J.; Watts, J. F. *Surf. Interface Anal.* **1994,** *21,* 263.
(11) Rutan, S. C.; Harris, J. M. *J. Chromatogr.* **1993,** *656,* 197.
(12) Wang, H.; Harris, J. M. *J. Am. Chem. Soc.* **1994,** *116,* 5754.
(13) Stahlberg, J.; Almgren, M.; Alsins, J. *Anal. Chem.* **1988,** *60,* 2487.
(14) Montgomery, M. E.; Green, M. A.; Wirth, M. J. *Anal. Chem.* **1992,** *64,* 1170.
(15) Zulli, S. L.; Kovaleski, J. M.; Zhu, X. R.; Harris, J. M.; Wirth, M. J. *Anal. Chem.* **1994,** *66,* 1708.
(16) Hansen, R. L.; Harris, J. M. *Anal. Chem.* **1995,** *67,* 492.
(17) Hansen, R. L.; Harris, J. M. *Anal. Chem.* **1996,** *68,* 2879.
(18) Wirth, M. J.; Burbage, J. D. *Anal. Chem.* **1991,** *63,* 1311.
(19) Burbage, J. D.; Wirth, M. J. *J. Phys. Chem.* **1992,** *96,* 5943.
(20) Wirth, M. J; Burbage, J. D.. *J. Phys. Chem.* **1992,** *96,* 9022.
(21) Piasecki, D. A.; Wirth, M. J. *J. Phys. Chem.* **1993,** *97,* 7700.
(22) Piasecki, D. A.; Wirth, M. J. *Langmuir* **1994,** *10,* 1913.
(23) Piasecki, D. A.; Montgomery, M. E.; Wirth, M. J. *Langmuir* **1995,** *11,* 990.
(24) Sassaman, J. L.; Wirth, M. J. *Colloids Surf.* **1994,** *93,* 49.
(25) Kovaleski, J. M.; Wirth, M. J. *J. Phys. Chem.* **1995,** *99,* 4091.
(26) Kovaleski, J. M.; Wirth, M. J. *J. Phys. Chem.* **1996,** *100,* 10304.
(27) Snyder, R. G.; Strauss, H. L.; Elliger, C. A. *J. Phys. Chem.* **1982,** *86,* 5145.
(28) Tamada, K.; Yu, H. *Langmuir* **1993,** *9,* 1545.
(29) Schlicht, L.; Ilgenfritz, G. *Physica A* **1996,** *227,* 239.
(30) Saxton, M. *Biophys. J.* **1982,** *39,* 165.
(31) Ali, J.; Andreoli-Bali, L.; Bhattacharyya, N.; Kronberg, B.; Patterson, D. *J. Chem. Soc., Faraday Trans. 1* **1985,** *81,* 3037.
(32) Lamotte, M.; Lesclaux, R.; Merle, A. M.; Joussot-Dubien, J. *Faraday Discuss. Chem. Soc.* **1974,** *58,* 253.